

On the checkerboard pattern and the autocorrelation of photoemission data in high temperature superconductors

E. Bascones and B. Valenzuela

*Instituto de Ciencia de Materiales de Madrid, CSIC. Cantoblanco. E-28049 Madrid, Spain**

(Dated: March 6, 2019)

In the pseudogap state the spectrum of the autocorrelation of angle resolved photoemission (AC-ARPES) data of $\text{Bi}_2\text{Sr}_2\text{CaCu}_2\text{O}_{8+\delta}$ presents non-dispersive peaks in momentum space which compare well with those responsible for the checkerboard pattern found in the density of states by Scanning Tunneling Microscopy. This similarity suggests that the checkerboard pattern originates from peaks in the joint density of states, as the dispersive peaks found in the superconducting state do. Here we show that the experimental AC-ARPES spectrum can be reproduced within a model for the pseudogap with no charge-ordering or symmetry breaking. We predict that, because of the competition of superconductivity and pseudogap, in the superconducting state, the AC-ARPES data of underdoped cuprates will present both dispersive and non-dispersive peaks and they will be better observed in cuprates with low critical temperature. We finally argue that the AC-ARPES data is a complementary and convenient way to measure the arc length.

In the pseudogap (PG) state of underdoped cuprates instead of a complete Fermi surface (FS)[1], just a Fermi arc around the nodal (diagonal) direction is seen, while the antinodal region close to $(\pi, 0)$ is gapped. Raman[2] and photoemission[3, 4, 5] experiments have shown that the nodal-antinodal dichotomy persists in the superconducting (SC) state, in the form of two different energy scales in nodal and antinodal regions. This behavior can be explained in terms of the coexistence and competition of SC and PG correlations below the critical temperature (T_c)[6]. The nature of the possible competing state remains controversial. Most of the proposals involve charge-ordering and/or breaking of the symmetry. To date there is no accepted evidence of such symmetry breaking. Strong support for charge-ordering models came from the observation of the so-called checkerboard pattern in Fourier Transform Scanning Tunneling Spectroscopy (FT-STs) measurements[7, 8, 9, 10, 11, 12, 13, 14, 15, 16]. But this interpretation seems at odds with the data obtained from the autocorrelation of the Angle Resolved Photoemission (ARPES) spectra[17, 18]. The checkerboard pattern refers to the non-dispersive peaks in the momentum \mathbf{q} and energy ω dependent density of states $n(\mathbf{q}, \omega)$ found at $\mathbf{q} \sim (\pm 2\pi/\lambda, 0)$ and $(0, \pm 2\pi/\lambda)$ with $\lambda \sim 4-5$ in units of the lattice spacing. Together with this modulation, weaker 3/4 substructure at $\mathbf{q} \sim (\pm(2\pi)3/4, 0)$ and $(0, \pm(2\pi)3/4)$ has been detected[11, 12, 13, 14, 15].

The lack of dispersion of the checkerboard peaks differentiate them from another kind of peaks also found by FT-STs in the SC state which disperse with binding energy. It is generally accepted that the dispersive features are a consequence of quantum interference of quasiparticles by elastic scattering[19, 20, 21]. In the quasiparticle interference picture, maxima in $n(\mathbf{q}, \omega)$ are expected at those momenta which connect the states with the largest joint density of states (JDOS). In the so-called octet model[19], in the SC state the largest density of states

at a given ω is found at the tips of the banana-shaped constant energy contours around the nodes (Fig. 1(a)) and $n(\mathbf{q}, \omega)$ peaks at the wavevectors $\mathbf{q}_1, \dots, \mathbf{q}_7$ which connect such tips. The size of these banana-shape constant energy contours changes with binding energy producing the dispersive behavior of the peaks. On the contrary, the origin of the checkerboard remains controversial and highly debated. Due to its non-dispersive nature[22], most of the models involve inhomogeneous states and charge ordering[11, 23, 24, 25, 26, 27, 28, 29, 30, 31, 32], but proposals based on the JDOS picture have been also discussed[22, 33].

The JDOS picture can be checked[34] autocorrelating ARPES data. The \mathbf{q} -space pattern measured from the autocorrelation of ARPES (AC-ARPES) data can be directly interpreted, as it does not require any theoretical modeling. Neglecting the matrix element, ARPES measures the spectral function $A(\mathbf{k}, \omega)$. In AC-ARPES the JDOS is obtained from the convolution

$$JDOS(\mathbf{q}, \omega) = \sum_{\mathbf{k}} A(\mathbf{k}, \omega) A(\mathbf{k} + \mathbf{q}, \omega). \quad (1)$$

The AC-ARPES spectra of $\text{Bi}_2\text{Sr}_2\text{CaCu}_2\text{O}_{8+\delta}$ (Bi2212) in the SC state[17, 18] show dispersive peaks as those expected from the octet model. In the PG state AC-ARPES data present[18] peaks near $(0.4\pi, 0)$ with very little dispersion, in contrast to the ones in the SC state. These non-dispersive peaks compare well with those responsible for the checkerboard in FT-STs. This similarity point to a JDOS explanation of the checkerboard and cast doubt on those models involving charge ordering. Analysis of the experimental data shows that they are associated to vectors of the \mathbf{q}_1^* type in Fig. 1(b), connecting the tips of the Fermi arcs. Peaks corresponding to \mathbf{q}_5^* in Fig. 1(b) and structure along the diagonal are also observed. It remains to be explained how does this non-dispersive behavior appears in the JDOS.

In this letter we show that the experimental AC-

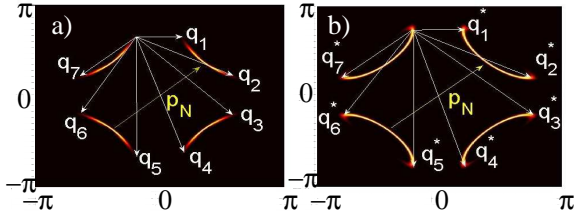


FIG. 1: (color online) (a) ARPES intensity around the nodes in the superconducting state for $\omega = -0.04$, in units of the bare nearest neighbor hopping, and $x = 0.20$. (b) Same as in (a) in the pseudogap state for $x = 0.16$ according to the model discussed. The wavevectors \mathbf{q}_i (\mathbf{q}_i^*) of quasiparticle interference patterns in the octet model, as well as the intranodal momenta along the diagonal \mathbf{P}_N .

ARPES spectrum is well reproduced by the model recently proposed by Yang, Rice and Zhang (YRZ) for the pseudogap[35]. Neither intrinsic charge-ordering or symmetry breaking are involved in this model or in the explanation of the experimental results. In agreement with experiments we find peaks with very little dispersion (referred as non-dispersive in the following) in the PG while clearly dispersive peaks appear in the SC state. This behavior is related to the different evolution of the constant energy contours size with binding energy and the existence of Fermi arcs at zero energy. Non-dispersive peaks presumably related to the checkerboard 3/4 substructure are also found in the PG. Furthermore, we predict that both dispersive and non-dispersive peaks can be present at low doping x in the SC state and we relate this result with the U-shape of the SC gap found in ARPES in underdoped SC cuprates[3, 36]. The dispersive ones are restricted to low energies, lower with underdoping. The non-dispersive features in the SC state dominate the spectrum at small doping and are a consequence of the persistence of PG correlations below T_c and its imprint on the spectral function and dispersion.

In the YRZ model PG correlations are given at zero temperature by Δ_R which does not break any symmetry because of its spin liquid origin[35]. Δ_R decreases with doping x and vanishes at a topological quantum critical point x_c . A crucial point in this model is the appearance of hole pockets close to $(\pm\pi/2, \pm\pi/2)$. Due to reduced spectral weight on the outer edge of the pocket, a gapless Fermi arc appears in ARPES at zero energy[6, 35]. At finite energy the arc structure remains as shown in Fig. 1(b).

In the SC state the SC order parameter Δ_S is related to T_c . It is assumed that PG and superconductivity coexist below T_c and x_c . Both Δ_R and Δ_S have d-wave symmetry $\Delta_\alpha(\mathbf{k}) = \Delta_\alpha(x)/2(\cos k_x - \cos k_y)$ with $\alpha = R, S$, but they gap the FS in a different way. At zero frequency the BCS self-energy diverges at the FS while the YRZ self-energy diverges at the umklapp surface $|k_x \pm k_y| = \pi$ [35]. Below x_c , we characterize the PG state by zero Δ_S and fi-

nite Δ_R . Beyond x_c , Δ_R vanishes and a complete Fermi surface and BCS behavior are recovered. We take the same parameters for Δ_S , Δ_R and the band dispersion proposed in the original paper[35] and used afterwards[6]. In particular, $\Delta_R(x)/2 = 0.3(1 - x/0.2)$ and $\Delta_S(x)/2 = 0.07(1 - 82.6(x - 0.2)^2)$ with energies units of the bare nearest neighbor hopping $t_0 \sim 300 - 400\text{meV}$. The anomalous behavior, i.e. the emergence of non-dispersive features, is expected below $x_c = 0.2$. The exact expressions for the spectral function and energies of the YRZ model have been given elsewhere[6, 35] and we do not repeat them here. To compare with experiments we calculate Eq. (1) following the same procedure[37] as in refs[17, 18]. Experimental AC-ARPES spectra is also influenced by the anisotropic and energy dependent lifetime not included here.

The AC-ARPES map in the SC state for $x_c = 0.20$ is shown in Fig. 2(a) $\omega = -0.04$. It closely resemble the one obtained from experimental data[17, 18] in the SC state, as well as those arising from the convolution of the Green function with itself discussed in the context of FT-STs experiments[19, 20] but it lacks the kaleidoscopic patterns due to umklapp[20, 37] present in the latest ones. The peaks corresponding to q_i -type terms in Fig. 1(a) are observed. The change of momenta with binding energy of the peaks along the bond and diagonal directions is clearly seen in Figs. 2(d) and 2(g). The almost dispersionless peak in Fig. 2(g). is due to nesting[20] and corresponds to \mathbf{P}_N -like contributions, as also seen by McElroy *et al*[17].

At first sight the ARPES intensities in the the BCS superconducting (Fig. 1(a)) and the PG states (Fig. 1(b)) look similar. But their AC-ARPES spectra and energy-dependence show important differences. Contrary to what happens in the SC case the peak along the bond in the AC-ARPES spectrum in the PG state is split in Fig. 2(e), *even at zero energy*. Their momenta and energy dependence resemble that found in the PG by Chatterjee *et al*[18]. Their positions change very little with energy in strong contrast to the dispersive behavior in Fig. 2(d). This weak dispersion could be reduced by finite lifetimes, weaker spectral weight at the antinode or worse experimental resolution than included here.

The checkerboard pattern is presumably related to the small momentum peak along the bond, \mathbf{q}_1^* . We note that the momentum at which the 3/4 substructure has been observed[11] is very close to that of the \mathbf{q}_5^* peak, and we postulate that both features are related. Zero-energy splitting and non-dispersing behavior also appear along the diagonal (Fig. 2(h)). The origin of the different behavior of peak position in the SC and PG states is related to the dependence of constant-energy contour size with binding energy which can be inferred from Fig. 2(j) and 2(k) where the corresponding energy spectrum along the $w = 0$ maximum ARPES intensity is reproduced. The length of the arrows at $w = -0.04$ and $w = -0.08$ give an

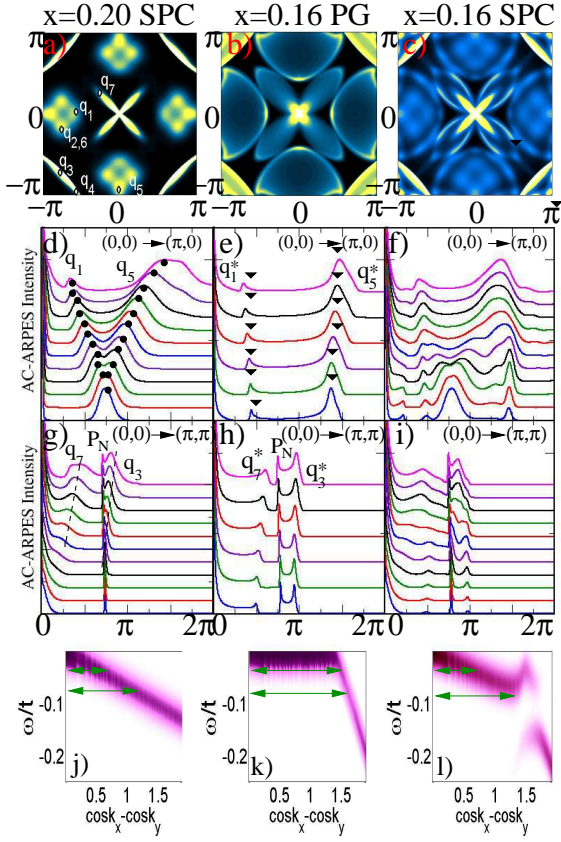


FIG. 2: (color online) AC-ARPES and energy spectra for $x_c = 0.20$ ($\Delta_R = 0, \Delta_S = 0.14$) in the superconducting state (left column) and $x_c = 0.16$ in the pseudogap state ($\Delta_R = 0.12, \Delta_S = 0$, middle column) and in the superconducting state ($\Delta_R = 0.12, \Delta_S = 0.12$, right column). (a) to (c) show, in arbitrary units, the maps at $\omega = -0.04$. (d) to (f), and (g) to (i) Intensity of the autocorrelated spectral function along the $(0,0) - (\pi,0)$ (bond) and $(0,0) - (\pi,\pi)$ (diagonal) directions respectively, at several energies. From bottom to top $\omega = 0$, to -0.10 in 0.02 intervals in the pseudogap state and in 0.01 intervals in the superconducting state, and in units of the bare nearest neighbor hopping. Each curve in (d) to (i) is normalized to the value at its largest feature other than the one at $(0,0)$ and displaced, to better show the peaks dispersion. The different behavior of the energy dispersion in the SC, PG and SC&PG states can be seen in (j) to (l) where the energy spectrum along the $w = 0$ maximum ARPES intensity line is plotted. Arrows are at $w = -0.04$ and $w = -0.08$.

idea on the change of the constant energy contours with binding energy. In the SC state the zero energy contour is a single point since all the FS is gapped. The contour size increases rapidly with binding energy. On the other hand, in the PG state the peak splitting along the bond comes from the finite size of the closed pocket centered around $(\pi/2\pi/2)$. The size of the constant-energy contour barely changes with binding energy.

Dispersive behavior at low energies appears in the SC state even for finite Δ_R . Interestingly, both dispersive and non-dispersive features can be distinguished

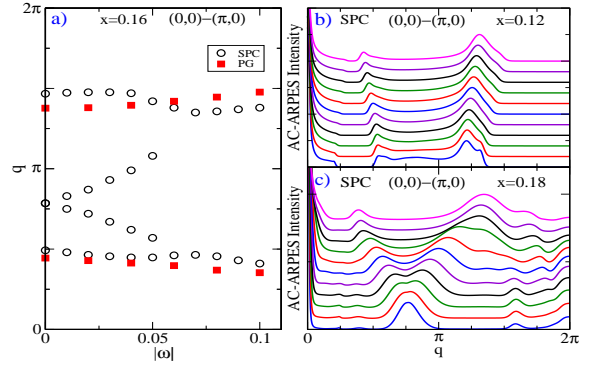


FIG. 3: (color online) (a) Position of the dispersing and non-dispersing peaks found in the $(0,0) - (\pi,0)$ direction in the superconducting and pseudogap state at $x = 0.16$. (b) and (c) Same as in Fig. 2(f) but for $x = 0.12$ ($\Delta_R = 0.24, \Delta_S = 0.07$) and $x = 0.18$ ($\Delta_R = 0.06, \Delta_S = 0.13$) respectively.

in Fig. 2(f). Dispersive peaks, of the type observed in Fig. 2(d), dominate at low energy but there is a clear kink in the dispersion and the peaks in the AC-ARPES spectrum converge to those observed in the PG state. The opening of a gap due to superconductivity in the arcs suppresses at low energies the non-dispersive peaks arising from the tips of the arcs but remanent structure is visible at the corresponding momenta. The appearance of both types of peaks is due to the coexistence of SC and PG. This coexistence can be seen in the energy band spectrum in Fig. 2(l). The gap in the arc at low energies is dominated by superconductivity. At higher energies, the antinodal region is mainly affected by the pseudogap. This energy spectrum has been proposed[6] to explain the U-shape of the SC gap found in ARPES in underdoped SC cuprates[3, 36]. The dispersive and non-dispersive features are better seen in Fig. 3(a), where the position of the maxima is plotted. The energy at which the change from dispersive to non-dispersive behavior happens is mainly given by $\Delta_S(\mathbf{k})$ at the arc tip, and depends on Δ_R , via the arc length. Overlap of dispersive and non-dispersive peaks does not always allow to differentiate them or to associate the position of the maximum in intensity to a particular kind of peak. We note that dispersive peaks at low energies and non dispersive ones at higher energies have been observed in FT-STs experiments in underdoped Bi2212[12]. The AC-ARPES spectra, corresponding to $x = 0.12$ and $x = 0.18$, in the SC state along the bond are shown in Figs. 3(b) and 3(c). Δ_S and Δ_R are finite in both cases. However, dispersive and non-dispersive peaks are not as clearly identified here as they were in Fig. 2(e). Thus the presence of only dispersive (non-dispersive) peaks does not guarantee zero Δ_R (Δ_S).

In general, for smaller $\frac{\Delta_S}{\Delta_R}$ the non-dispersive structure is more pronounced and for a given doping, the range of energies at which dispersive features appear is reduced

with decreasing Δ_S . In agreement with recent ARPES measurements[5], we expect Δ_S to be to some extent related to T_c . Based on this argument, we predict that in the SC state the peaks in the AC-ARPES spectra of low T_c cuprates, like $\text{Ca}_{2-x}\text{Na}_x\text{CuO}_2\text{Cl}_2$ (Na-CCOC) or $\text{Bi}_2\text{Sr}_2\text{CuO}_{6+\delta}$ (Bi2201), will be mostly non-dispersive, similar to the ones found in the PG state in Bi2212[18]. In low T_c cuprates Δ_R and Δ_S are expected to differ more and $\frac{\Delta_S}{\Delta_R}$ to be smaller. We note that in FT-STs experiments in the SC state, the checkerboard pattern is better seen in cuprates with low T_c and when the integrated density of states lacks the coherence peaks, when it is more PG like[11, 12, 14, 15]. In fact, to the best of our knowledge in FT-STs dispersive features in the SC state have been seen so far only in Bi2212[8, 9, 12], and not in low- T_c cuprates as Na-CCOC[11] or $\text{Bi}_2\text{Sr}_{1.6}\text{La}_{0.4}\text{CuO}_{6+\delta}$ (Bi2201-La)[15]. The observation of dispersive peaks at very low energies in FT-STs experiments has been maybe prevented by the small signal-to-noise ratio at low energies. On the other hand, ARPES measurements work well at these energies. Confirmation of the presence of both dispersive and non-dispersive peaks in AC-ARPES in the SC state (with the dispersive ones restricted to energies of a few meV in some cases) would confirm the existence of two energy scales and a common origin of the peaks observed in AC-ARPES and FT-STs.

Recent ARPES experiments[38] have suggested that in the PG state the Fermi length is temperature dependent and vanishes at low temperatures, while the antinodal region remains gapped up to the PG temperature. The arc length, as measured directly from the ARPES intensity suffers from large uncertainty. The observation by Chatterjee *et al*[18] that the nondispersive peaks found in the AC-ARPES in the PG state arise from the tips of the Fermi arcs and that a SC-type gap in the arcs results in dispersive features, opens a new way to get complementary information on the length of the Fermi arc. We propose that AC-ARPES experiments can be used to determine the position of the arc tips and nodal Fermi momentum, as well as of the arc length and its dependence with temperature and doping. We note that as the spectra is autocorrelated the uncertainty of the position of the arc tips is strongly reduced compared to the bare intensity. The dependence of the arc size with energy can be also measured, providing extra information of the physics involved in the truncation of the Fermi surface. We believe that low T_c cuprates are the most suitable for this experiment as the two energy scales Δ_R and Δ_S will be most different and underdoped non-SC samples, showing the checkerboard, are available[11].

In conclusion, we have shown that the non-dispersive structure found in the autocorrelation of photoemission data in Bi2212 in the pseudogap state can be explained without involving charge ordering or symmetry breaking but the existence of the Fermi arcs and a weak binding energy dependence of the size of the constant energy con-

tour. We believe that both the checkerboard and its 3/4 substructure can be explained within a joint density of states picture. Furthermore, we predict the simultaneous appearance of both dispersing and non-dispersing peaks in the AC-ARPES spectra in the superconducting state of underdoped cuprates which originates in the U-shape of the SC gap, and will be better observed in materials with low T_c . The observation of the coexistence of the two-types of peaks would be the *smoking gun* which confirm the joint density of states mechanism for the checkerboard, the equivalence of AC-ARPES and FT-STs peaks and the coexistence of pseudogap and superconductivity below x_c . We also propose to autocorrelate ARPES data to measure the arc length and its temperature dependence.

After the first submission of this work we have been aware of new experimental results with confirm the prediction of coexistence of dispersing and non-dispersing peaks in the superconducting state[39].

We acknowledge funding from MEC through Grant No. FIS2005-05478-C02-01 and Ramon y Cajal contract and from Consejería de Educación de la Comunidad de Madrid and CSIC through Grant No. 200550M136 and I3P contract.

* Electronic address: leni@icmm.csic.es, belenv@icmm.csic.es

- [1] M.R. Norman *et al.*, Nature **392**, 157 (1998).
- [2] M. Le Tacon *et al.*, Nature Physics **2**, 138 (2006).
- [3] K. Tanaka *et al.*, Science **314**, 1910 (2006).
- [4] M. Hashimoto *et al.*, cond-mat/0610758.
- [5] T. Kondo *et al.*, cond-mat/0611517.
- [6] B. Valenzuela and E. Bascones, Phys. Rev. Lett. **98**, 227002 (2007).
- [7] J.E. Hoffman *et al.*, Science **295**, 466 (2002).
- [8] J.E. Hoffman *et al.*, Science **297**, 1148 (2002).
- [9] K. McElroy *et al.*, Nature (London) **422**, 592 (2003).
- [10] M. Vershinin *et al.*, Science **303**, 1995 (2004).
- [11] T. Hanaguri *et al.*, Nature (London) **430**, 1001 (2004).
- [12] K. McElroy *et al.*, Phys. Rev. Lett. **94**, 197005 (2005).
- [13] G. Levy *et al.*, Phys. Rev. Lett. **95**, 257005 (2005).
- [14] A. Hashimoto *et al.*, Phys. Rev. B **74**, 064508 (2006).
- [15] T. Machida *et al.*, J. Phys. Soc. Japan **75**, 083708 (2006).
- [16] C. Howald *et al.*, Phys. Rev. B **67**, 014533 (2003).
- [17] K. McElroy *et al.*, Phys. Rev. Lett. **96**, 067005 (2006).
- [18] U. Chatterjee *et al.*, Phys. Rev. Lett. **96**, 107006 (2006).
- [19] Q.-H. Wang and D.-H. Lee, Phys. Rev. B **67**, 020511 (2003).
- [20] L. Capriotti, D.J. Scalapino and R.D. Sedgewick, Phys. Rev. B **68**, 014508 (2003). T. Peregr-Barnea and M. Franz, Phys. Rev. B **68**, 180506 (2003).
- [21] L. Zhu, W.A. Atkinson and P.J. Hirschfeld **69**, 060503 (2004). T. Nunner *et al.*, Phys. Rev. B **73**, 104511 (2006).
- [22] Misra *et al.*, Phys. Rev. B, **70**, 220503 (2004).
- [23] H.-D. Chen *et al.*, Phys. Rev. Lett. **89**, 137004 (2002).
- [24] Z. Tesanovic, Phys. Rev. Lett. **93**, 217004 (2004).
- [25] A. Polkovnikov, M. Vojta and S. Sachdev, Phys. Rev. B **65**, 220509 (2002).

- [26] D. Podolsky *et al*, Phys. Rev. B **67**, 094514 (2003).
- [27] M. Vojta, Phys. Rev. B **66**, 104505 (2002).
- [28] P.W. Anderson, cond-mat/0406038.
- [29] F.J. Ohkawa, Phys. Rev. B **73**, 092506 (2006).
- [30] C. Li *et al*, Phys. Rev. B **73**, 060501 (2006).
- [31] J.X Li, C.Q Wu, D.H. Lee, Phys. Rev. B **74**, 184429 (2006).
- [32] L. Dell'Anna *et al*, Phys. Rev. B **71**, 064518 (2005).
- [33] C. Bena *et al*, Phys. Rev. B **69**, 134517 (2004). A. Ghosal, A. Kopp, S. Chakravarty, Phys. Rev. B **72**, 220502 (2005).
- [34] R.S. Markiewicz Phys. Rev. B **69**, 214517 (2004).
- [35] K-Y Yang, T.M. Rice and F-C Zhang, Phys. Rev. B **73**, 174501 (2006).
- [36] J. Mesot *et al*, Phys. Rev. Lett. **83**, 840 (1999).
- [37] Only those momenta \mathbf{k} which satisfy that both \mathbf{k} and $\mathbf{k}+\mathbf{q}$ belong to the first Brillouin zone are included in the sum. Umklapp terms do not enter and the autocorrelated spectra does not have the lattice symmetry. To mimic finite energy-resolution in ARPES, the spectral function is convoluted with a gaussian of width $0.02t_0$.
- [38] A. Kanigel *et al*, Nature Phys. **2**, 447 (2006).
- [39] U. Chatterjee *et al*, cond-mat/0705.4136.